

## LUNAR OPPOSITION EFFECT AS INFERRED FROM HIGH-RESOLUTION LRO CAMERA DATA.

K. Sysoliatina<sup>1</sup>, A. Razim<sup>1</sup>, V. Kaydash<sup>1</sup>, Y. Shkuratov<sup>1</sup>, G. Videen<sup>2</sup>, <sup>1</sup>Astronomical Institute of Kharkov National University, Sumskaia 35, Kharkov, 61022 Ukraine, sskevja@yandex.ua, <sup>2</sup>Space Science Institute, 4750 Walnut St. Suite 205, Boulder, CO 80301, USA.

**Introduction:** The lunar opposition effect (brightness surge observed at phase angles  $\alpha$  close to zero) remains a subject of great interest because the phase function  $f(\alpha)$  describing this effect depends on surface properties, e.g., on the size of regolith particles and the regolith porosity [e.g., 1]. An important problem, when one calculates the phase curve from images, is that the data statistics or reliability of phase curve determination decreases rapidly with decreasing  $\alpha$ . This is a consequence of the finiteness of spatial resolution of imaging cameras onboard orbital lunar spacecraft. At present, photometric data of the highest spatial resolution (about 0.5 m/pixel) are provided by the NAC LROC instrument [2]. This suggests a unique opportunity to retrieve from images the lunar phase curves at very small phase angles  $<1^\circ$ . At this range the effect of phase function smoothing by the Sun disk [3-5] is feasible for the Moon.

**Processing the NAC LROC data:** To extract phase curve from reflectance images one should separate albedo variations over the scene and the opposition spike pattern itself. We used phase ratios method that is suitable for this aim [1,4,6]. It implies producing the ratio of two images of the same scene. The first of them contains the zero-phase-angle point, the second one is taken at a larger phase angle. This procedure almost eliminate albedo pattern on the resulting image. The processing of NAC images includes converting raw data into radiance factor, selenographic reference and calculation of photometric angles [1] for each pixel in the frames. For this we use the ISIS software [7] with latest SPICE kernels [8].

**Calculation of phase functions:** To derive a phase function we performed: (1) registering two suitable images with sub-pixel accuracy; (2) obtaining the phase ratio image by dividing their corresponding pixels; (3) division of the ratio image into bins of a constant phase angle and averaging values inside each bin. Small phase angle variations are used to produce the bins; such variations related to the image acquired at larger phase angles are eliminated at in-bin averaging. When performing the step (3) we masked in the phase-ratio image small topographic features (bright walls and shadows of the craters) that spoil the image due to substantial variations of local illumination/emission angles. Thus, we removed undesirable pixels from further analysis.

For instance, Fig. 1 illustrates results of the described steps: (a) the reflectance image M109311328L (width of the strip is 2.5 km), (b) the phase angle ratio M109311328L/M172995906R corresponding on average to  $f(0^\circ)/f(15^\circ)$ , (c) the phase angle distribution for the image M109311328L. The phase-ratio image includes the opposition area (bright vertical portion); the albedo pattern here is almost removed. Phase angle variations in the frame of M172995906R are small and as has been noted their effect was taken into account at in-bin averaging.

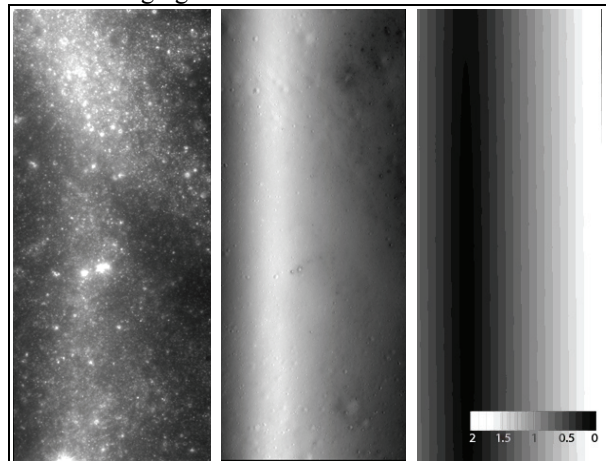


Figure 1. Left to right: Image M109311328L with opposition area, phase ratio image ( $0^\circ/15^\circ$ ) and low-phase-angle distribution. North is up .

The same sense procedure was carried out for the image pair M171685902R ( $\alpha \sim 0^\circ$ ) and M141030879R ( $\alpha \sim 6^\circ$ ). Thus we analyzed phase functions for two near-equatorial lunar sites (Table 1 shows selenographic coordinates of the point  $\alpha=0$ ). Site 1 is a highland near the lunar farside center, while site 2 is a mare surface in Procellarum.

Site	Image ID	Longitude	Latitude
1	M171685902R	187.95	-1.55
2	M109311328L	348.14	-1.46

**Discussion:** Figure 2 presents phase curves for two sites obtained with an angular resolution of  $0.01^\circ$ . Both curves are normalized to their own values at  $\alpha=0.5^\circ$ . Due to high spatial resolution of NAC the number of pixels falling in each  $0.01^\circ$  bin varies from  $10^4$  (at  $\alpha \sim 0^\circ$ ) to  $10^5$  (at  $\alpha \sim 0.7^\circ$ ) providing high data accuracy. The phase function  $f(\alpha)$  of highlands reveals stronger

opposition effect (higher slope) as compared to the mare surface (cf. experimental curves in Fig. 2).

*Phase curve flattening due to angular size of the Sun.* Measurements of bidirectional reflectance in classical planetary photometry imply a point-like light source and detector separated by the phase angle. However, in case of the Moon we cannot consider the Sun as a point due to its finite angular size equal  $0.5^\circ$  at 1 a.u. Each point of the Sun's disk is an independent light source that has its own phase angle. Thus the observed disk phase curve (d-curve) is a sum of great number of point curves (p-curves). As a result of such a summing, one should expect some flattening of a d-curve at small angles  $\alpha < 0.5^\circ$  [1,3-5]. In Fig. 2 this effect can be seen at small angles for mare and highland d-curves.

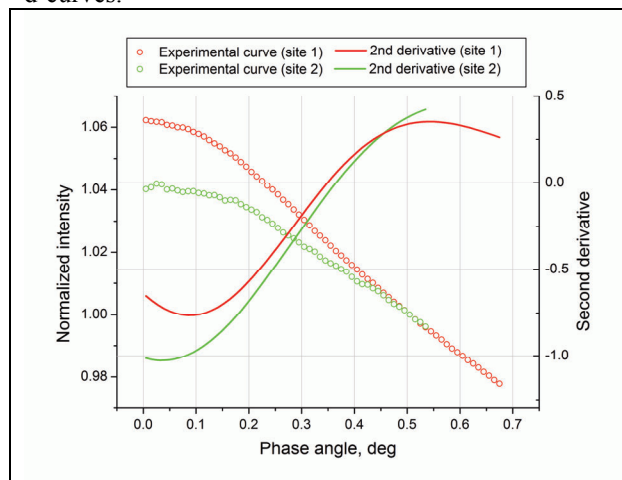


Figure 2. Experimental phase curves and their second derivatives for highland (1) and mare (2) sites

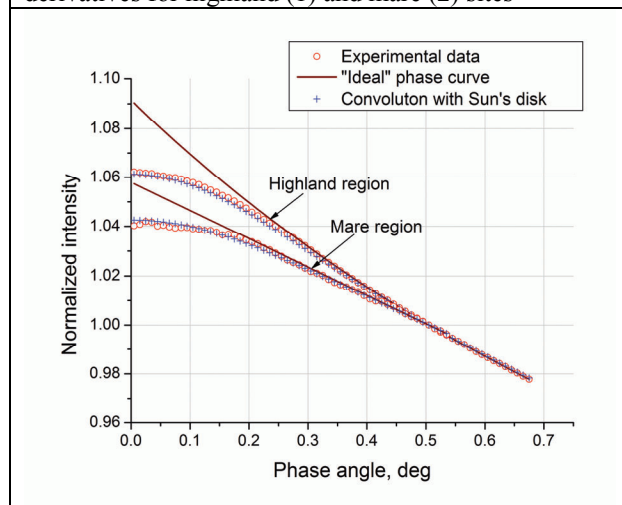


Figure 3. Experimental phase curves, p-curves, and their convolution with the distribution of brightness over Sun's disk [10]

The angle corresponding to the curve inflection depends on the width and amplitude of the opposition

surge. To determine the angle, we fitted experimental phase curves using the least square method with a simple function  $f = c_1 \exp(-k_1 \alpha^2 - k_2 \alpha) + c_2$ , where  $c_1$ ,  $c_2$ ,  $k_1$ , and  $k_2$  are fitting parameters. Using this function we plotted the second derivative for the mare and highland phase curves (see Fig. 2). We found that the inflection ( $f'' = 0$ ) occurs at  $\alpha_1 = 0.36^\circ$  and  $\alpha_2 = 0.37^\circ$  for the curves 1 and 2 in Fig. 2, respectively.

*Restoring p-curves from d-curves.* Strictly speaking such a restoration is an ill-posed problem that does not have the exact solution. One may suggest an approximate analysis of the problem using two assumptions. First, we consider that due to low albedo the Moon in the NAC spectral range does not have a narrow opposition spike related to the coherent backscattering enhancement [1]. Second, we describe the shadow effect with the linear-exponential function  $f = b_0 + b_1 \alpha + \exp(-\alpha/2w)$  [5, 9]. We used this function varying its parameters for the convolution with a kernel modeling the solar disk and solar limb darkening [10]. Solid curves in Fig. 3 present the best found p-curves, open circles correspond to experimental data, and pluses are results of convolution of the p-curves with the solar disk function. Our results show very good agreement between experimental curves and the result of convolution. This allows us to make sure that our two assumptions are valid and found "extrapolation" of lunar phase p-curves at the range  $< 1^\circ$  is correct.

**Conclusions:** Using NAC LROC data we obtained phase curves for two lunar sites with high phase-angle resolution. New phase functions allow studying the opposition effect for phase angles as low as  $0.01^\circ$ . We found the phase curve inflection at angles  $0.36-0.37^\circ$ ; this is a consequence of the angular size of the Sun. Our modeling allows us to restore p-curves (for mare and highland areas) using experimental NAC LROC data.

**References:** [1] Shkuratov Y. et al. (2011) *Planet. Space Sci.*, 59, 1326-1371. [2] Robinson M. et al. (2010) *Space Sci. Rev.* 150, 81-124. [3] Shkuratov Y. (1991) *Solar System Res.* 25, 54-57. [4] Shkuratov Y. et al. (1999) *Icarus* 141, 132-155. [5] Déau E. (2013) *Icarus*, 226, 1465-1488. [6] Kaydash V. et al. (2012) *J. Quant. Spectrosc. Radiat. Trans.* 113, 2601-2607. [7] [isis.astrogeology.usgs.gov](http://isis.astrogeology.usgs.gov). [8] [naif.jpl.nasa.gov/pub/naif/pds/data/lro-l-spice-6-v1.0/lrosp\\_1000](http://naif.jpl.nasa.gov/pub/naif/pds/data/lro-l-spice-6-v1.0/lrosp_1000). [9] Velikodsky Y. et al. (2011) *Icarus* 214, 30-45. [10] Allen C.W., (1973) *Astrophysical Quantities*, Athlone Press, London.